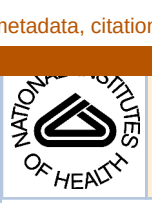

Published in final edited form as:

Clin Cancer Res. 2008 September 1; 14(17): 5416–5425. doi:10.1158/1078-0432.CCR-08-0150.

Inhibition of the p53 E3 Ligase HDM-2 Induces Apoptosis and DNA Damage-Independent p53 Phosphorylation in Mantle Cell Lymphoma

Richard J. Jones[1], **Qing Chen**[2], **Peter M. Voorhees**[2], **Ken H. Young**[3], **Nathalie Bruey-Sedano**[4], **Dajun Yang**[4], and **Robert Z. Orlowski**[1,5]

1*The Department of Lymphoma and Myeloma, University of Texas M. D. Anderson Cancer Center, Houston, TX*

2*Lineberger Comprehensive Cancer Center, University of North Carolina at Chapel Hill, Chapel Hill, NC*

3*University of Wisconsin School of Medicine and Public Health, Madison, WI*

4*Ascenta Therapeutics Inc., San Diego, CA*

5*Department of Experimental Therapeutics, University of Texas M. D. Anderson Cancer Center, Houston, TX.*

Abstract

Purpose—The ubiquitin-proteasome pathway has been validated as a target in non-Hodgkin lymphoma through demonstration of the activity of the proteasome inhibitor bortezomib.

Experimental Design—Another potentially attractive target is the human homologue of the murine double minute-2 protein, HDM-2, which serves as the major p53 E3 ubiquitin ligase, and we therefore evaluated the activity of a novel agent, MI-63, which disrupts the HDM-2/p53 interaction.

Results—Treatment of wild-type p53 mantle cell lymphoma cell lines (MCL) with MI-63 resulted in a dose- and time-dependent inhibition of proliferation, with an IC_{50} in the 0.5-5.0 μM range. MI-63 induced p53 and HDM-2 accumulation, as well as other downstream p53 targets such as p53-upregulated modulator of apoptosis and $p21^{Cip1}$. This was associated with cell cycle arrest at G_1/S, activation of caspases-3, -8 and -9, cleavage of poly-(ADP-ribose) polymerase, and loss of E2F1. HDM-2 inhibition caused phosphorylation of p53 at multiple serine residues, including 15, 37 and 392, which coincided with low levels of DNA strand breaks. DNA damage occurred in a small percentage of cells, and did not induce phosphorylation of the DNA damage marker $H2A.X^{Ser139}$. Combinations of MI-63 with the molecularly targeted agents bortezomib and rapamycin showed synergistic, sequence-dependent anti-proliferative effects. Treatment of primary MCL patient samples resulted in apoptosis and induction of p53 and p21, which was not seen in normal controls.

Conclusions—These findings support the hypothesis that inhibition of the HDM-2/p53 interaction may be a promising approach both by itself, and in combination with currently used chemotherapeutics, against lymphoid malignancies.

Keywords

HDM-2; MDM-2; mantle cell lymphoma; MI-63; nutlin; p53

Address correspondence to: Dr. Robert Z. Orlowski, The University of Texas M. D. Anderson Cancer Center, Department of Lymphoma and Myeloma, 1515 Holcombe Blvd., Unit 429, Houston, TX 77030-4009; Telephone: 713-792-2860; Fax: 713-563-5067; Email: rorlowsk@mdanderson.org.

Introduction

Non-Hodgkin lymphomas (NHL) are a complex group of lymphoid malignancies showing a wide range of pathobiology and clinical behavior (1). Mantle cell lymphoma (MCL) is a distinct NHL subgroup accounting for 6-8% of all lymphoid malignancies, which displays the immunophenotype of a B-cell lymphoma (2,3). At the molecular level, MCL is characterized by the presence of an 11;14 translocation resulting in the overexpression of Cyclin D1. Clinically, MCL presents in elderly patients and follows an aggressive course, with relapse occurring almost invariably despite good initial outcomes to conventional chemotherapies (2). One recent encouraging development has been the approval of the proteasome inhibitor bortezomib (VELCADE®) after demonstration of its clinical activity in the relapsed/refractory setting (4-6). This agent has helped to validate the ubiquitin-proteasome pathway as a target for NHL therapy, and pre-clinically resulted in part in accumulation of p53, and down-stream targets such as $p21^{Cip1}$ (7).

Another mechanism by which p53 turnover can be impacted is by targeting p53 ubiquitination, a necessary precursor prior to its proteasome-mediated degradation. The murine double minute (MDM)-2 protein, and its human homologue, HDM-2, are the major E3 ligases responsible for p53 ubiquitination (8). HDM-2 is an oncogene that is over-expressed in a variety of malignancies, including leukemias, sarcomas, and solid tumors (9), and may play a role in NHL as well (10). In addition to its E3 ligase activity, HDM-2 also inhibits p53 function through binding to the NH_2-terminus of p53 and suppressing its transcriptional activation properties (8). Under conditions of cellular stress, the ability of HDM-2 to bind p53 is blocked, preventing HDM-2 from inhibiting p53 function. This results in a rise in p53 levels, cell cycle arrest, induction of apoptosis, and senescence (11,12).

Small molecule inhibitors of the interaction between HDM-2 and p53 such as nutlin restore p53 function in tumor cells with *wtp53* (13,14). Nutlin binds in the p53-binding pocket of HDM-2 and displaces p53, resulting in stabilization of p53, p21 expression, cell cycle arrest, apoptosis and growth inhibition (13). These effects were found to be specific for malignancies with *wtp53*, did not induce p53 phosphorylation, and had a limited effect on primary cells. Recent work has found that, although nutlin acts through the HDM-2/p53 interaction, other cellular targets have been identified, including the cell cycle regulator E2F1 (15), the androgen receptor (16), hypoxia-inducible factor (17), and the nuclear factor-κB pathway (18). The potential to target the HDM-2/p53 interaction has not been evaluated in models of NHL, however, and given the above rationale, its potential utility in MCL was of interest.

Materials and Methods

Reagents

The HDM-2 inhibitor MI-63 was provided by Ascenta Therapeutics, Inc. Nutlin-3 (NUT), mechlorethamine (MCT), doxorubicin (DOX), pifithrin-α (PIFT), and rapamycin (RAP) were purchased from Sigma-Aldrich, while bortezomib (BZB) and cisplatin (CISP) were from the University of North Carolina clinical pharmacy.

Cell culture and patient samples

JVM-2, GRANTA-519, REC-1, Jeko-1, Karpas-422, BL-41, and WSU-NHL cells were purchased from the German Collection of Microorganisms and Cell Cultures, while CCRF-CEM were purchased from the American Type Culture Collection. Cells were grown in RPMI 1640 (Invitrogen) supplemented with 10% fetal bovine serum (Sigma-Aldrich), 100 U/ml penicillin, and 100 μg/ml streptomycin, except GRANTA-519, which were grown in DME-M (Invitrogen). Patient samples were collected and purified as previously described (19).

Semi-Quantitative RT-PCR

Total RNA was isolated using an RNeasy Plus kit (Qiagen) and cDNA was synthesized using Superscript II (Invitrogen). PCR was performed for 30 cycles, unless indicated otherwise, for p53-upregulated modulator of apoptosis (PUMA; GenBank™ accession number: NM_014417) using sense primer 5′-CGGCGGAGACAAGAGGAGCA-3′ and antisense primer 5′-GTGAAGGAGCACCGAGAGGAGA-3′. Primers and conditions for $p21^{Cip1}$ and β_2-microglobulin (β_2M) were as previously described (20,21).

Immunoblot

Protein expression in drug-treated cells was measured by immunoblot analysis performed as previously described (21). Antibodies to p53, HDM-2, E2F1, and ubiquitin were purchased from Santa Cruz Biotechnologies, while anti-phospho-p53 and anti-poly-(ADP-ribose) polymerase (PARP) antibodies were from Cell Signaling Technologies and anti-β-Actin was from Sigma-Aldrich.

Cell cycle analysis

Cells were treated with drug for 24 hours, then fixed and stained with propidium iodide (Sigma-Aldrich). Cell cycle data were analyzed on a FacsCalibur (Becton-Dickson) using FlowJo v. 6.3.3 (Tree Star, Inc.).

Flow cytometry

Levels of total p53, phospho-Ser15-p53, H2A.X-Ser139 and cleaved caspase-3 were measured by flow cytometry after cells were fixed in paraformaldehyde and then permeabilized in 100% methanol. Antibodies to cleaved caspase-3 and H2A.X-Ser139 were purchased from Cell Signaling Technologies.

ELISA for p21 and phospho-p53-Ser15

Cells were treated with vehicle control, 5μM MI-63, nutlin, or 0.5μM DOX. ELISAs were performed using a p21 (Assay Designs) or a phospho-p53-Ser15 ELISA kit (Cell Signaling Technology) according to the manufacturer's instructions. p21 levels were expressed in μg/ml calculated from the recommended standard curve, while the fold induction in phospho-p53-Ser-15 content was determined from the absorbance values and normalized to untreated controls from triplicate experiments.

Caspase activation assay

Activation of caspases was evaluated in cell lysates as previously described (19). The pan-caspase inhibitor Z-VAD and caspase-8 and -9 inhibitors were purchased from Calbiochem and used at concentrations of 50μM.

DNA damage assays

Cells were treated as indicated in the text, and DNA damage was measured using the Trevigen Comet Assay Kit. Apurinic and apyrimidinic DNA damage was measured using the DNA Damage Quantification Kit (Biovision).

Cell proliferation assay

The WST-1 reagent (Roche Diagnostics) was used to determine the effects of HDM-2 inhibitors on cell proliferation and their relative IC_{50} as previously published (19).

Drug synergy assays

To evaluate for the presence of synergistic interactions, the methods of Chou and Talalay were used (22,23). Briefly, MI-63, DOX, CISP, BZB, or RAP were added to cells, and the IC_{50} of each drug individually was determined using the WST-1 assay. The calculated IC_{50} was then designated 1xIC_{50}, and similar determinations were made at 0.25x, 1x, 2x, and 4x the IC_{50}. MI-63 and the other chemotherapy drugs were used in a 1:1 ratio and added simultaneously to the cells for 3 days and WST-1 assays were performed. Data were then analyzed using CalcuSyn software (Biosoft), and combination indices (CI) were calculated.

Results

MI-63 inhibits the growth of NHL cell lines

The HDM-2 inhibitor MI-63 has been shown to bind HDM-2 *in vitro* with a K_i of 3 nM, and was effective in the activation of p53 resulting in inhibition of growth of epithelial cancer cell lines (24,25). To evaluate its impact on NHL, cell lines of varying p53 status (Supplementary Table 1) were treated with MI-63 for 3 days, and IC_{50} values were calculated using a cell viability assay. MCL cell lines with wild-type p53 (*wtp53*; JVM-2, Granta-519 and REC-1) were sensitive to MI-63, with IC_{50} values ranging from 0.79-1.12 μM (Fig.1A, left). However, an MCL cell line with mutant p53 (*mutp53*; Jeko-1) was relatively resistant, with an IC_{50} of almost 12 μM. A second panel of cells representing different NHL histologies was also studied (Fig.1A, right), and three of the *mutp53* cell lines (CCRF-CEM, BL-41 and KARPAS-422) were again relatively resistant to MI-63. Interestingly, the *mutp53* Waldenström's cell line WSU-NHL was sensitive, with an IC_{50} of 1.95μM.

HDM-2 inhibition should stabilize p53 and induce up-regulation of HDM-2, since it is itself a p53 target. MCL *wtp53* cell lines treated with MI-63 for 24 hours indeed revealed an increase in total p53 levels (Fig.1B and supplementary Fig.1) similar to that seen with doxorubicin, while no change was seen in *mutp53* Jeko-1 cells. HDM-2 levels increased significantly in MI-63-treated JVM-2 and Granta-519 cells, though only a slight increase was noted in REC-1 cells, and no change was seen in Jeko-1 cells. To determine if these findings correlated with triggering of apoptosis, the late stage apoptosis marker PARP was studied, and found to be cleaved in *wtp53* MCL lines at concentrates equal to or greater than 5μM.

We also examined the effect of MI-63 on p53 in the *mutp53* lines, and in the two where p53 was detectable, WSU-NHL and CCRF-CEM, total p53 levels did not change significantly (Fig. 1B and supplementary Fig.1). No HDM-2 expression was seen in either Jeko-1 or WSU-NHL cells, but in CCRF-CEM cells, MI-63 induced a paradoxical decrease in HDM-2 levels. A noticeable effect was seen on PARP in the CCRF-CEM and WSU-NHL cell lines, where MI-63 at 5μM and greater induced cleavage that was equivalent to, or greater than that seen with doxorubicin. This lack of change in p53 levels with continued induction of PARP cleavage may point to the presence of p53-independent mechanisms of action for HDM-2 inhibitors in these cell backgrounds.

Given the possible relevance of p53-independent mechanisms, it was of interest to determine if any of the mechanism of action of MI-63 was dependent on functional *wtp53*. Pifithrin-α inhibits p53-dependent transcription and p53-mediated apoptosis (26), and should therefore reverse some of the effects of MI-63 treatment of *wtp53* cells. Indeed, Granta-519 cells exposed to PIFT in combination with MI-63 were partially rescued from cell death (Fig.1C), and a similar effect was seen with nutlin. Thus, p53-dependent mechanisms are important to the mechanism of action of these HDM-2 inhibitors. The incomplete rescue may indicate another secondary, p53-independent mechanism may also be active, or incomplete suppression of p53 by PIFT in these experiments.

MI-63 induces upregulation of p53 target genes

We next examined the ability of MI-63 to upregulate the downstream p53 target genes *p21* and *PUMA* by evaluating their transcript levels with RT-PCR. Both *p21* and *PUMA* increased in response to MI-63 in the *wtp53* MCL cell lines (Fig.2A and supplementary Fig.2A). The *mutp53* WSU-NHL had a small increase in *p21* and *PUMA* by RT-PCR (Fig.2A and supplementary Fig.2A), but no change was seen in Jeko-1 or CCRF-CEM. p21 protein levels were measured with a quantitative ELISA to determine if this increased transcript level resulted in increased protein abundance. Protein lysates from MCL, WSU-NHL and CCRF-CEM that had been treated with MI-63 demonstrated that *wtp53* MCL cells had an increase in p21 protein, which was especially marked in JVM-2 cells (Fig.2B). In contrast, *mutp53* Jeko-1, WSU-NHL and CCRF-CEM cells demonstrated little to no baseline p21 expression, and no increase with MI-63.

The HDM-2 inhibitor nutlin has previously been shown to induce cell cycle arrest (13,16,27, 28), so we examined NHL cells treated with MI-63 for a similar effect. *wtp53* MCL cells showed a G_1/S cell cycle arrest after 5μM MI-63, with REC-1 cells being the most affected (Fig.2C). Jeko-1 and WSU-NHL *mutp53* cells had no evidence of cell cycle arrest, but they did arrest in G_2/M after treatment with DOX (Supplementary Fig.2B). These results suggested that MI-63 acted similarly to nutlin in its ability to induce p21 and a G_1/S cell cycle arrest.

MI-63 induces caspase-mediated cell death

To further define the mechanism of cell death in MI-63-exposed cells, we measured caspase-3, -8, and -9 activities in MI-63-treated MCL cells. All *wtp53* MCL cells had an increase in caspase-3 activity, ranging from a 3-fold increase in REC-1, to an 8-fold increase in JVM-2 (Fig.3A). This was associated with an increase in caspase-8 activity to some extent in all of these cells, particularly REC-1, and may indicate a death receptor-mediated mechanism of cell death. Caspase-9 activation was more variable, and seen predominantly in REC-1, while *mutp53* Jeko-1 cells, in contrast, showed little if any activation of these caspases. The incubation of the pan-caspase inhibitor Z-VAD with MI-63 resulted in a partial rescue of cell death in REC-1 (Supplementary Fig.3A), and a similar effect was seen with nutlin. Inhibition of caspases-8 and -9 individually in cells treated with either MI-63 or nutlin showed little to no ability to rescue cell viability.

The time course of caspase-3 induction was also measured in JVM-2 and REC-1 cells. Caspase-3 activity began to rise 3 hours after addition of MI-63, peaked after 12 hours, and then began to fall, whereas activity in DOX-treated cells continued to increase up to 24 hours in JVM-2 (Fig.3B). REC-1 cells showed a slower onset of caspase-3 activation in that levels did not rise until 6 hours after addition of MI-63 or DOX, then peaked at 12 hours, and began to fall at 24 hours for both agents (Supplementary Fig.3B). Accumulation of p53 was also rapid following MI-63 treatment in both cell lines, with increased p53 levels seen as early as 3 hours, which continued to be elevated above baseline even after 24 hours (Fig.3C and supplementary Fig.3C). We also noticed that the abundance of the cell cycle regulator E2F1 decreased after addition of MI-63 after 3 hours, and was lost almost completely by 12 and 24 hours in JVM-2 and REC-1 cells, respectively.

HDM-2 inhibitors induce p53 phosphorylation

Interference with the HDM-2/p53 interaction by nutlins has previously been shown to induce cell death in the absence of genotoxic effects as measured by the phosphorylation status of p53 at Serine-15 (13). It was therefore of interest to determine if this was also the case in our MCL models, since it could indicate that adding genotoxic drugs such as alkylating agents to HDM-2 inhibitors may enhance anti-NHL activity. Notably, treatment with both MI-63 and nutlin resulted in the appearance of p53 phosphorylated at serines-15, -37, and -392 (Fig.4A), though

to a lesser extent than with the known genotoxic agent DOX. Since ataxia telangiectasia-mutated (ATM) protein kinase is responsible for phosphorylation of p53 at serines-15 and -37 in response to DNA damage, we determined its expression levels. No change in the abundance of total ATM was detected after treatment with MI-63 or nutlin, nor was there any alteration of expression of activated ATM, which is phosphorylated at Ser-1981.

To further investigate the phosphorylation of p53, we quantitatively measured phospho-p53-Ser-15 levels by an ELISA. The *wtp53* cells JVM-2, GRANTA-519, and REC-1 each had increases in phospho-p53 abundance (Supplementary Fig.4A), ranging from a two to three-fold increase in REC-1 and Granta-519, to a 14-fold increase in JVM-2. In addition, the time course of p53 phosphorylation was studied, and phospho-p53-Ser-15 levels rose as early as 3 hours after exposure to MI-63 (Supplementary Fig.4B), as was the case for total p53 levels. Levels peaked at 6-12 hours after exposure, at which time the first evidence of PARP cleavage was seen.

As p53 phosphorylation is associated with damage to DNA (reviewed in (29)), we used the comet assay to determine whether HDM-2 inhibition was inducing DNA damage. JVM-2 cells treated with DOX suffered extensive DNA damage as indicated by the development of large comet tails (Fig.4B). While MI-63 and nutlin did not induce comet tails to the same extent, MI-63 did nonetheless produce a halo effect around cells, suggesting the presence of early DNA damage that was not seen after vehicle treatment. To further evaluate for the presence of DNA damage, we next studied cells for the presence of apurinic and apyrimidinic (AP) DNA lesions formed during base excision and repair of oxidized, deaminated, or alkylated bases. JVM-2 cells treated with MI-63 were found to contain 2.0×10^5 AP lesions per base pair (Supplementary Fig.4C), compared to 3.7×10^5 AP lesions for cells treated with the alklyating agent mechlorethamine. Interestingly, no increase in AP lesions was seen in nutlin-treated cells, and may indicate an off-target effect for MI-63.

To further characterize the p53-phosphorylation and apparent DNA damage *in situ*, we combined phospho-Ser15-p53 or total p53 immunostaining with either cleaved caspase-3, or the surrogate DNA double strand break marker phospho-H2AX (30,31). In JVM-2, neither MI-63 nor nutlin induced a significant increase in H2AX expression compared to vehicle-treated cells, despite inducing strong caspase-3 cleavage (Fig.4C, top panel). Moreover, this H2AX expression was not linked to expression of phospho-Ser-15-p53 (Fig.4C, middle panel), with only 7% of cells expressing both p53-phospho-Ser-15 and H2AX after treatment with MI-63 or nutlin. In contrast, cisplatin treatment resulted in 46% of cells expressing both p53-phospho-Ser-15 and H2AX. These results were further confirmed by evaluating total p53 and H2AX (Fig.4C, lower panel), which showed that total p53 levels increased in response to MI-63 or nutlin, while little to no increase was seen in the number of cells expressing H2AX compared to cisplatin. These findings indicate that low levels of DNA damage occurred in a small percentage of cells after HDM-2 inhibition, but the damage was not significant enough to elicit DNA response pathways as measured by ATM and H2AX phosphorylation.

MI-63 synergizes with other molecularly targeted therapeutics

Given the finding that HDM-2 inhibition resulted in little to no DNA damage, it was of interest to determine if the activity of these agents *in vitro* could be augmented by DNA damaging drugs. We combined MI-63 with either cisplatin or doxorubicin using JVM-2 as a model system. Under some conditions, there did appear to be an additive impact on JVM-2 viability (Fig.5). Interestingly, interaction analysis failed to show combination indices documenting synergy (Table 1). Two other agents that have recently shown promise against MCL are the targeted drugs bortezomib (BZB) and rapamycin (RAP)(32). Enhanced anti-proliferative activity was seen with the MI-63 and rapamycin combination, and also with MI-63 and bortezomib (Fig.5). Interaction analysis showed that both RAP and BZB were synergistic with

MI-63 over all IC_{50} doses, and this synergy was especially marked with RAP, while the BZB synergy was weaker (Table 1).

The effectiveness of combination chemotherapy may in some cases depend upon the order of drug administration (33). We therefore examined whether MI-63 would be more or less effective at inhibiting cell proliferation depending upon the exposure sequence to other chemotherapeutics. Pretreatment of JVM-2 with the IC_{50} of MI-63, followed 24 hours later by addition of the IC_{50} of DOX, CISP, BZB, or RAP, was not more effective at inhibiting proliferation than MI-63 alone (Supplementary Fig.5). However, pretreatment with the IC_{50} of the chemotherapeutic for 24 hours followed by the IC_{50} of MI-63 for 24 hours was far more efficient at inhibiting cell growth. The proteasome inhibitor BZB was particularly effective at inhibiting cell growth in this assay. Pretreatment of cells with MI-63 followed by chemotherapy resulted in lower levels of p53 accumulation due to the low IC_{50} doses used compared to MI-63 alone (Supplementary Fig.5), whereas when the chemotherapeutic was given first and then followed by MI-63, the ability of MI-63 to induce p53 was restored. Notably, neither DOX nor CISP in combination with MI-63 was more effective at inducing p53 expression compared to MI-63 alone when the chemotherapeutic agent was given second. However, when MI-63 was given after the chemotherapeutic agent, p53 accumulation was markedly enhanced. Similar findings were seen with BZB and RAP, which induced greater expression of p53 only when cells were exposed first to these agents and then later to MI-63 (Supplementary Fig.5).

MI-63 effects in patient-derived samples

As inhibition of HDM-2 function in MCL cell culture models showed promising efficacy, we evaluated the ability of MI-63 and nutlin to affect normal peripheral blood mononuclear cells (PBMCs) and lymphoma cells. Peripheral blood from normal healthy donors and a newly diagnosed patient with blastoid MCL (MCL-1) were purified, and treated with a range of doses of MI-63 or nutlin. Both agents inhibited the growth of MCL cells, with IC_{50} values of 6.4 and 7.6μM, respectively (Fig.6A). In contrast, neither agent reached its IC_{50} against the normal PBMC samples, even at doses up to 100μM, suggesting a degree of selectivity for malignant cells. Finally, incubation of MCL-1 with MI-63 or nutlin resulted in the accumulation of p53 and an increase in p21 expression (Fig.6B), even in the absence of a clear increase in HDM-2. Notably, both nutlin and MI-63 were more effective at inducing p53 and p21 than doxorubicin.

Discussion

MCL is an aggressive B-cell lymphoproliferative disorder in which standard chemotherapeutic regimens have limited efficacy, in that though they can induce remissions these responses are typically short-lived (34,35). The inability to cure MCL has accelerated research into the field of molecularly targeted drugs that may have enhanced efficacy with manageable side effect profiles. Oncotherapeutics often harness the ability of cells to induce apoptosis in response to DNA damage, but genotoxic agents frequently result in non-specific side effects with selection of drug-resistant clones. One encouraging development has been the approval of the proteasome inhibitor bortezomib, which functions in part by inducing accumulation of p53 and p21, as well as other downstream p53 targets. In addition, the nongenotoxic activation of apoptosis through exploitation of a functional p53 pathway and the use of HDM-2 inhibitors has been shown to be an effective apoptosis-inducing strategy for solid tumor malignancies (13), as well as hematologic malignancies such as multiple myeloma (36). Thus, our goal was to evaluate the potential activity of such inhibitors as therapeutics in models of lymphoma.

In this work we have examined the effects of a novel inhibitor of the HDM-2/p53 interaction, MI-63, and compared its efficacy to another agent in this class, nutlin, in a panel of NHL cell lines, normal $CD19^+$ B-cells, and an MCL patient sample. MCL lines with *wtp53* were sensitive to the effects of MI-63, as were patient-derived lymphoma cells, while normal PBMCs were

much more resistant, supporting the possibility of an acceptable therapeutic index. *wtp53* MCL cell lines treated with HDM-2 inhibitors activated a p53-mediated gene expression program, became arrested at G_1/S, and were induced to undergo programmed cell death.

The HDM-2 inhibitor nutlin was originally shown to induce effects consistent with p53 accumulation, but without any effects on p53 phosphorylation (13). Our data demonstrate, however, that both nutlin and MI-63 induce p53 phosphorylation in the MCL models used in our study. These findings are consistent with those of Secchiero and colleagues, who reported p53 phosphorylation at Ser-15 in B-cell chronic lymphocytic leukemia samples after exposure to nutlin (37). Similarly, weak p53 phosphorylation was seen recently in Hodgkin Reed-Sternberg cells (27). Since previous work with nutlins in epithelial cancer cell lines showed no p53 phosphorylation (38), one interpretation is that these effects are specific to lymphoid cells. However, very recent publications have demonstrated the presence of p53 phosphorylation in mouse embryonic fibroblasts at Ser-18 (39), the human homologue of phospho-Ser-15-p53, and in primary kidney cells (40) after treatment with nutlin. Thus, it seems likely that this may prove to be not just a cell-type, but even a cell-line-dependent effect.

Phosphorylation of p53 at serine-15 and -37 is typically the result of both genotoxic and non-genotoxic insults. Genotoxic stresses include topoisomerase II inhibitors, nitric oxide, hydrogen peroxide, ultraviolet light, and ionizing radiation (29), while non-genotoxic insults include severe hypoxia and replicative senescence (29). In the comet assay, we did not observe clear comet tails that would indicate DNA damage, and only a small amount of damage was seen with MI-63 in the context of AP lesions. Moreover, this only induced H2AX in a small percentage of cells, suggesting that the phosphorylation changes were largely due to nongenotoxic mechanisms. One possibility is that the increase in phospho-Ser-15-p53 and phospho-Ser-37-p53 levels may be due to an increase in total p53, which is then phosphorylated to the same extent as in inhibitor-naïve cells, but more readily detected due to a greater abundance. Indeed, densitometric scanning of immunoblots was supportive of this hypothesis (data not shown). However, the increase in phospho-Ser-392-p53 is important since this increases p53 tetramerization, and its ability to bind its consensus DNA sequence (41), thereby promoting its ability to induce transactivation (42). Further studies will be needed to determine the extent to which these phosphorylation status alterations reflect true changes in p53 function, and whether these contribute to the apoptotic process.

HDM-2 inhibition in MCL was more effective in suppressing proliferation in JVM-2, Granta-519, and REC-1 cells, which have *wtp53*, compared with Jeko-1, which has *mutp53*. As expected, *mutp53* Karpas-422 diffuse large cell lymphoma cells were among the most resistant to MI-63, and this supports the role of *wtp53* as the mechanism responsible for MI-63 in this cell type. A surprising finding was that MI-63 was quite potent against the *mutp53* WSU-NHL Waldenström's cell line, and also active, albeit with an intermediate IC_{50}, against *mutp53* CCRFCEM acute lymphoblastic leukemia cells. On the mechanistic side, this suggests that such inhibitors are disrupting HDM-2-mediated pathways that are independent of p53. This idea is supported by our data with pifithrin-α , which was unable to give a complete rescue from nutlin or MI-63 in *wtp53* cells. Differential effects of nutlin have been reported in cell lines with mutant and wild-type p53 in respect to the modulation of E2F1 when nutlin was combined with CISP (15). Our results in *mutp53* cells did not require another drug, however, and we did not observe a decrease in E2F1 in *mutp53* cells (data not shown), as we did for the *wtp53* cells. We did observe an increase in p21 activation by RT-PCR in WSU-NHL cells, which did not result in p21 protein expression, but could indicate that p73 may be acting in these cells to induce cell death. In this regard, nutlin has previously been shown to disrupt HDM-2/p73 interactions in *wtp53*, *mutp53*, and p53-null cells (43). However, recent studies suggest that nutlin can have pleiotropic effects, including on pathways such as angiogenesis (17), androgen signaling (16), and nuclear factor-κB (18). Thus, a number of candidate

pathways will need to be studied to determine those that most contribute to the activity of these agents in *mutp53* NHL models. Also of note, MI-63 and nutlin do differ in their structures, and while both bind residues Phe-19, Trp-23, and Leu-26 of the p53/HDM-2 interacting domain, MI-63 also captures a fourth residue, Leu-22, which may play an important role in the interaction between HDM-2 and p53 (24,44,45). This may allow MI-63 to serve as a more potent inhibitor of the p53/HDM2 interaction as compared to nutlin, and may also allow it to extend effects to *mutp53* cells. We are in the process of generating cell lines resistant to MI-63, which should aid in identifying at least some of these pathways, and may also guide the development of future combination regimens based on these drugs.

From a clinical perspective, the validation of a new target as being of potential interest for lymphoma therapy is encouraging, and the current findings support studies of HDM-2 inhibitors in patients with relapsed and/or refractory NHL. Combination chemotherapy is typically a far more effective treatment modality than single agents, however, and we indeed found that combining MI-63 with rapamycin or bortezomib displayed increased synergy compared to conventional chemotherapeutics. Pretreatment with MI-63 was antagonistic to chemotherapy, which is consistent with other published works demonstrating that pre-treatment of *wtp53* tumors actually protected the cells from chemotherapy-mediated toxicity. However, similar pretreatment in *mutp53* cell lines induced greater levels of apoptosis (46). Interestingly, other work has demonstrated that nutlin is protective for kidney cells receiving CISP therapy, and this protection appears independent of the HDM-2, HDM-4, or p53 status of the cells (40). The potential clinical effectiveness of MI-63 is also bolstered by a recent study of the *in vivo* form of this drug, MI-219, which was shown to be active in murine xenograft models with an excellent side effect profile (25). Moreover, MI-219 plasma levels of greater than 13μM were achieved following a single oral dose of 50mg/kg in mice (25), which are above those which were needed in our MCL and NHL models. Taken together, these findings support the translation of HDM-2 inhibitors such as MI-63 into the clinic both as single agents, and in combination with other chemotherapeutics using a rational sequence of administration that may be influenced by p53 status, for the treatment of lymphoid malignancies.

Supplementary Material

Refer to Web version on PubMed Central for supplementary material.

Acknowledgements

The authors would like to thank Drs. George Small and Deborah Kuhn for useful discussions, and help with manuscript preparation. R.Z.O., a Leukemia & Lymphoma Society Mansbach Foundation Scholar in Clinical Research, would also like to acknowledge support from the Leukemia & Lymphoma Society (6096-07), and the National Cancer Institute (RO1 CA102278).

References

1. Jaffe, ESHN.; Stein, H.; Vardiman, JW., editors. World Health Organisation of Classification of Tumours. Lyon: 2001. Pathology and genetics of tumours and lymphoid tissues; p. 168-70.
2. Campo E, Raffeld M, Jaffe ES. Mantle-cell lymphoma. Semin Hematol 1999;36:115–27. [PubMed: 10319380]
3. Swerdlow SH, Williams ME. From centrocytic to mantle cell lymphoma: a clinicopathologic and molecular review of 3 decades. Hum Pathol 2002;33:7–20. [PubMed: 11823969]
4. Orlowski RZ, Stinchcombe TE, Mitchell BS, et al. Phase I trial of the proteasome inhibitor PS-341 in patients with refractory hematologic malignancies. J Clin Oncol 2002;20:4420–7. [PubMed: 12431963]

5. O'Connor OA, Wright J, Moskowitz C, et al. Phase II clinical experience with the novel proteasome inhibitor bortezomib in patients with indolent non-Hodgkin's lymphoma and mantle cell lymphoma. J Clin Oncol 2005;23:676–84. [PubMed: 15613699]
6. Goy A, Younes A, McLaughlin P, et al. Phase II study of proteasome inhibitor bortezomib in relapsed or refractory B-cell non-Hodgkin's lymphoma. J Clin Oncol 2005;23:667–75. [PubMed: 15613697]
7. Perez-Galan P, Roue G, Villamor N, Montserrat E, Campo E, Colomer D. The proteasome inhibitor bortezomib induces apoptosis in mantle-cell lymphoma through generation of ROS and Noxa activation independent of p53 status. Blood 2006;107:257–64. [PubMed: 16166592]
8. Haupt Y, Maya R, Kazaz A, Oren M. Mdm2 promotes the rapid degradation of p53. Nature 1997;387:296–9. [PubMed: 9153395]
9. Momand J, Jung D, Wilczynski S, Niland J. The Mdm2 gene amplification database. Nucleic Acids Res 1998;26:3453–9. [PubMed: 9671804]
10. Finnegan MC, Goepel JR, Royds J, Hancock BW, Goyns MH. Elevated levels of Mdm-2 and p53 expression are associated with high grade non-Hodgkin's lymphomas. Cancer Lett 1994;86:215–21. [PubMed: 7982210]
11. Lane DP. Cancer. p53, guardian of the genome. Nature 1992;358:15–6. [PubMed: 1614522]
12. Levine AJ. p53, the cellular gatekeeper for growth and division. Cell 1997;88:323–31. [PubMed: 9039259]
13. Vassilev LT, Vu BT, Graves B, et al. *In vivo* activation of the p53 pathway by small-molecule antagonists of Mdm2. Science 2004;303:844–8. [PubMed: 14704432]
14. Issaeva N, Bozko P, Enge M, et al. Small molecule Rita binds to p53, blocks p53-Hdm-2 interaction and activates p53 function in tumors. Nat Med 2004;10:1321–8. [PubMed: 15558054]
15. Ambrosini G, Sambol EB, Carvajal D, Vassilev LT, Singer S, Schwartz GK. Mouse double minute antagonist Nutlin-3a enhances chemotherapy-induced apoptosis in cancer cells with mutant p53 by activating E2F1. Oncogene 2007;26:3473–81. [PubMed: 17146434]
16. Logan IR, McNeill HV, Cook S, Lu X, Lunec J, Robson CN. Analysis of the Mdm2 antagonist Nutlin-3 in human prostate cancer cells. Prostate 2007;67:900–6. [PubMed: 17440969]
17. LaRusch GA, Jackson MW, Dunbar JD, Warren RS, Donner DB, Mayo LD. Nutlin3 blocks vascular endothelial growth factor induction by preventing the interaction between hypoxia inducible factor 1alpha and Hdm2. Cancer Res 2007;67:450–4. [PubMed: 17234751]
18. Dey A, Wong ET, Bist P, Tergaonkar V, Lane DP. Nutlin-3 inhibits the NFkappaB pathway in a p53-dependent manner: implications in lung cancer therapy. Cell Cycle 2007;6:2178–85. [PubMed: 17786042]
19. Kuhn DJ, Chen Q, Voorhees PM, et al. Potent activity of carfilzomib, a novel, irreversible inhibitor of the ubiquitin-proteasome pathway, against preclinical models of multiple myeloma. Blood 2007;110:3281–90. [PubMed: 17591945]
20. Ookawa K, Kudo T, Aizawa S, Saito H, Tsuchida S. Transcriptional activation of the Muc2 gene by p53. J Biol Chem 2002;277:48270–5. [PubMed: 12374798]
21. Jones RJ, Dickerson S, Bhende PM, Delecluse HJ, Kenney SC. Epstein-Barr virus lytic infection induces retinoic acid-responsive genes through induction of a retinol-metabolizing enzyme, Dhrs9. J Biol Chem 2007;282:8317–24. [PubMed: 17244623]
22. Chou, TC. The median-effect principle and the combination index for quantitation of synergism and antagonism. In: Chou, TC.; Rideout, DC., editors. Synergism and antagonism in chemotherapy. Academic Press; San Diego: 1991. p. 61-102.
23. Chou TC, Talalay P. Quantitative analysis of dose-effect relationships: the combined effects of multiple drugs or enzyme inhibitors. Adv Enzyme Regul 1984;22:27–55. [PubMed: 6382953]
24. Ding K, Lu Y, Nikolovska-Coleska Z, et al. Structure-based design of spiro-oxindoles as potent, specific small-molecule inhibitors of the Mdm2-p53 interaction. J Med Chem 2006;49:3432–5. [PubMed: 16759082]
25. Shangary S, Qin D, McEachern D, et al. Temporal activation of p53 by a specific Mdm2 inhibitor is selectively toxic to tumors and leads to complete tumor growth inhibition. Proc Natl Acad Sci USA 2008;105:3933–8. [PubMed: 18316739]
26. Komarov PG, Komarova EA, Kondratov RV, et al. A chemical inhibitor of p53 that protects mice from the side effects of cancer therapy. Science 1999;285:1733–7. [PubMed: 10481009]

27. Drakos E, Thomaides A, Medeiros LJ, et al. Inhibition of p53-murine double minute 2 interaction by Nutlin-3a stabilizes p53 and induces cell cycle arrest and apoptosis in Hodgkin lymphoma. Clin Cancer Res 2007;13:3380–7. [PubMed: 17545546]
28. Graat HC, Carette JE, Schagen FH, et al. Enhanced tumor cell kill by combined treatment with a small-molecule antagonist of mouse double minute 2 and adenoviruses encoding p53. Mol Cancer Ther 2007;6:1552–61. [PubMed: 17513604]
29. Lavin MF, Gueven N. The complexity of p53 stabilization and activation. Cell Death Differ 2006;13:941–50. [PubMed: 16601750]
30. Bewersdorf J, Bennett BT, Knight KL. H2AX chromatin structures and their response to DNA damage revealed by 4Pi microscopy. Proc Natl Acad Sci USA 2006;103:18137–42. [PubMed: 17110439]
31. Thiriet C, Hayes JJ. Chromatin in need of a fix: phosphorylation of H2AX connects chromatin to DNA repair. Mol Cell 2005;18:617–22. [PubMed: 15949437]
32. Hipp S, Ringshausen I, Oelsner M, Bogner C, Peschel C, Decker T. Inhibition of the mammalian target of rapamycin and the induction of cell cycle arrest in mantle cell lymphoma cells. Haematologica 2005;90:1433–4. [PubMed: 16219581]
33. Mitsiades N, Mitsiades CS, Richardson PG, et al. The proteasome inhibitor PS-341 potentiates sensitivity of multiple myeloma cells to conventional chemotherapeutic agents: therapeutic applications. Blood 2003;101:2377–80. [PubMed: 12424198]
34. Bertoni F, Zucca E, Cotter FE. Molecular basis of mantle cell lymphoma. Br J Haematol 2004;124:130–40. [PubMed: 14687022]
35. Bosch F, Lopez-Guillermo A, Campo E, et al. Mantle cell lymphoma: presenting features, response to therapy, and prognostic factors. Cancer 1998;82:567–75. [PubMed: 9452276]
36. Stuhmer T, Chatterjee M, Hildebrandt M, et al. Nongenotoxic activation of the p53 pathway as a therapeutic strategy for multiple myeloma. Blood 2005;106:3609–17. [PubMed: 16081689]
37. Secchiero P, Barbarotto E, Tiribelli M, et al. Functional integrity of the p53-mediated apoptotic pathway induced by the nongenotoxic agent Nutlin-3 in B-cell chronic lymphocytic leukemia (B-CLL). Blood 2006;107:4122–9. [PubMed: 16439677]
38. Thompson T, Tovar C, Yang H, et al. Phosphorylation of p53 on key serines is dispensable for transcriptional activation and apoptosis. J Biol Chem 2004;279:53015–22. [PubMed: 15471885]
39. Efeyan A, Ortega-Molina A, Velasco-Miguel S, Herranz D, Vassilev LT, Serrano M. Induction of p53-dependent senescence by the Mdm2 antagonist Nutlin-3a in mouse cells of fibroblast origin. Cancer Res 2007;67:7350–7. [PubMed: 17671205]
40. Jiang M, Pabla N, Murphy RF, et al. Nutlin-3 protects kidney cells during cisplatin therapy by suppressing Bax/Bak activation. J Biol Chem 2007;282:2636–45. [PubMed: 17130128]
41. Hupp TR, Meek DW, Midgley CA, Lane DP. Regulation of the specific DNA binding function of p53. Cell 1992;71:875–86. [PubMed: 1423635]
42. Yap DB, Hsieh JK, Zhong S, et al. Ser392 phosphorylation regulates the oncogenic function of mutant p53. Cancer Res 2004;64:4749–54. [PubMed: 15256442]
43. Lau LM, Nugent JK, Zhao X, Irwin MS. Hdm2 antagonist Nutlin-3 disrupts p73-Hdm2 binding and enhances p73 function. Oncogene 2007;27:997–1003. [PubMed: 17700533]
44. Lin J, Chen J, Elenbaas B, Levine AJ. Several hydrophobic amino acids in the p53 amino-terminal domain are required for transcriptional activation, binding to Mdm-2 and the adenovirus 5 E1B 55-kD protein. Genes Dev 1994;8:1235–46. [PubMed: 7926727]
45. Picksley SM, Vojtesek B, Sparks A, Lane DP. Immunochemical analysis of the interaction of p53 with Mdm2;--fine mapping of the mdm-2 binding site on p53 using synthetic peptides. Oncogene 1994;9:2523–9. [PubMed: 8058315]
46. Carvajal D, Tovar C, Yang H, Vu BT, Heimbrook DC, Vassilev LT. Activation of p53 by Mdm2 antagonists can protect proliferating cells from mitotic inhibitors. Cancer Res 2005;65:1918–24. [PubMed: 15753391]

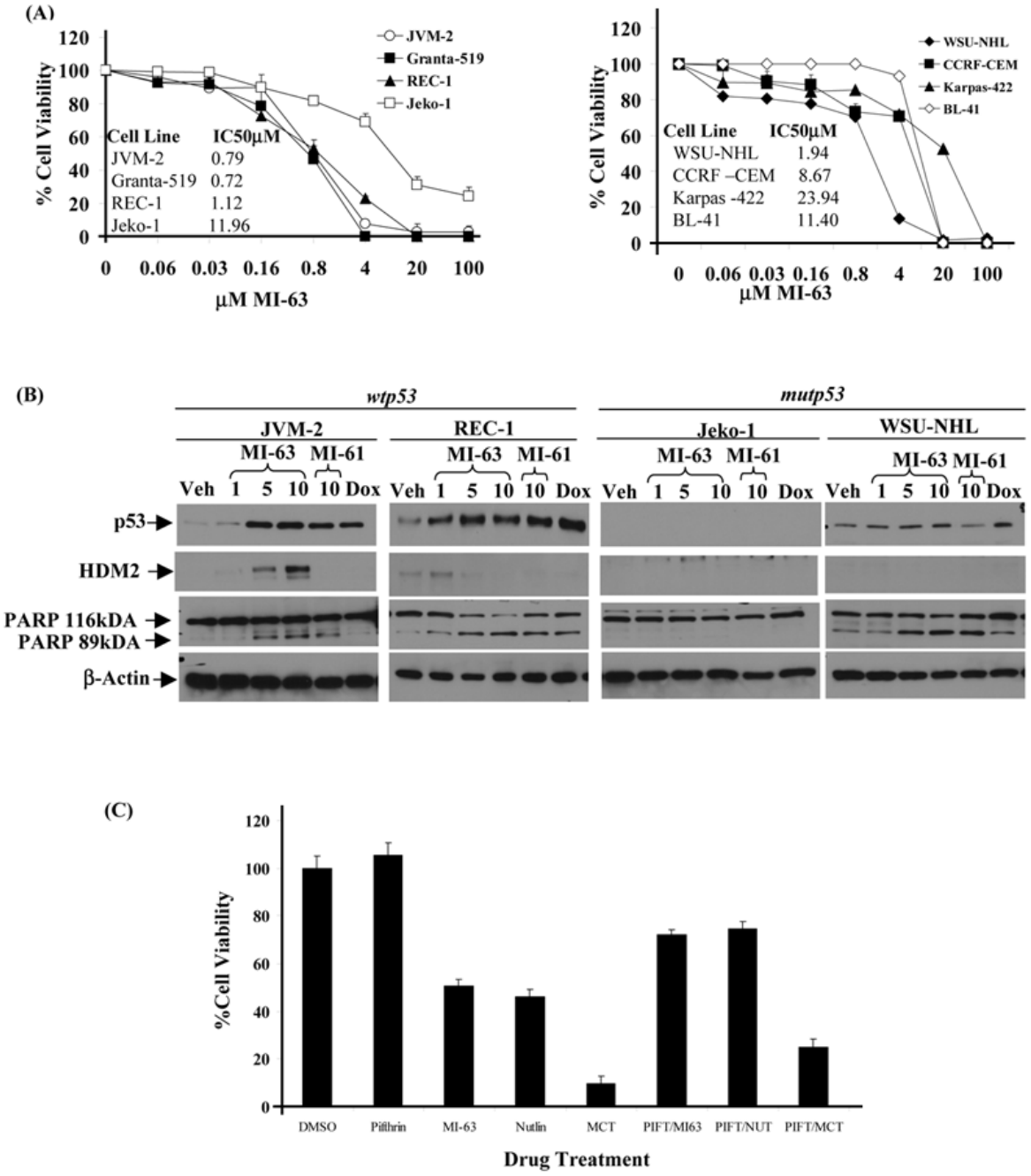

Figure 1. MI-63 inhibits the proliferation of non-Hodgkin lymphoma cell lines

(A) Cells were seeded in 96-well plates for viability analysis using the WST-1 reagent, and treated with the indicated doses of MI-63 for 72 hours. WST-1 results are expressed as the percentage cell viability in relation to the vehicle-treated sample for each cell line, which was arbitrarily set at 100%. Experiments were performed in triplicate, and mean values with the standard error of the mean (SEM) are shown. (B) For immunoblot analysis, cells were seeded in 6-well plates and treated with the indicated concentrations of MI-63, vehicle, or 0.5μM doxorubicin for 24 hours. Extracts were then probed for their content of p53, HDM-2, PARP, and β-Actin as a loading control. A representative Western blot is shown of the triplicate experiments performed. PARP cleavage is seen at higher concentrations of MI-63 than the

IC_{50} identified in panel A because the former assays were performed for 72-hours, while the latter were for only 24-hours, thereby requiring greater drug concentrations to induce the same effect. (C) Granta-519 cells were treated with 10μM of the p53 inhibitor pifithrin-α alone, or in combination with either 5μM MI-63, nutlin, or 10μM MCT as a positive control for 24 hours. Cell viability was determined using a WST-1 viability assay. All experiments shown were performed in triplicate and mean values are shown along with the SEM.

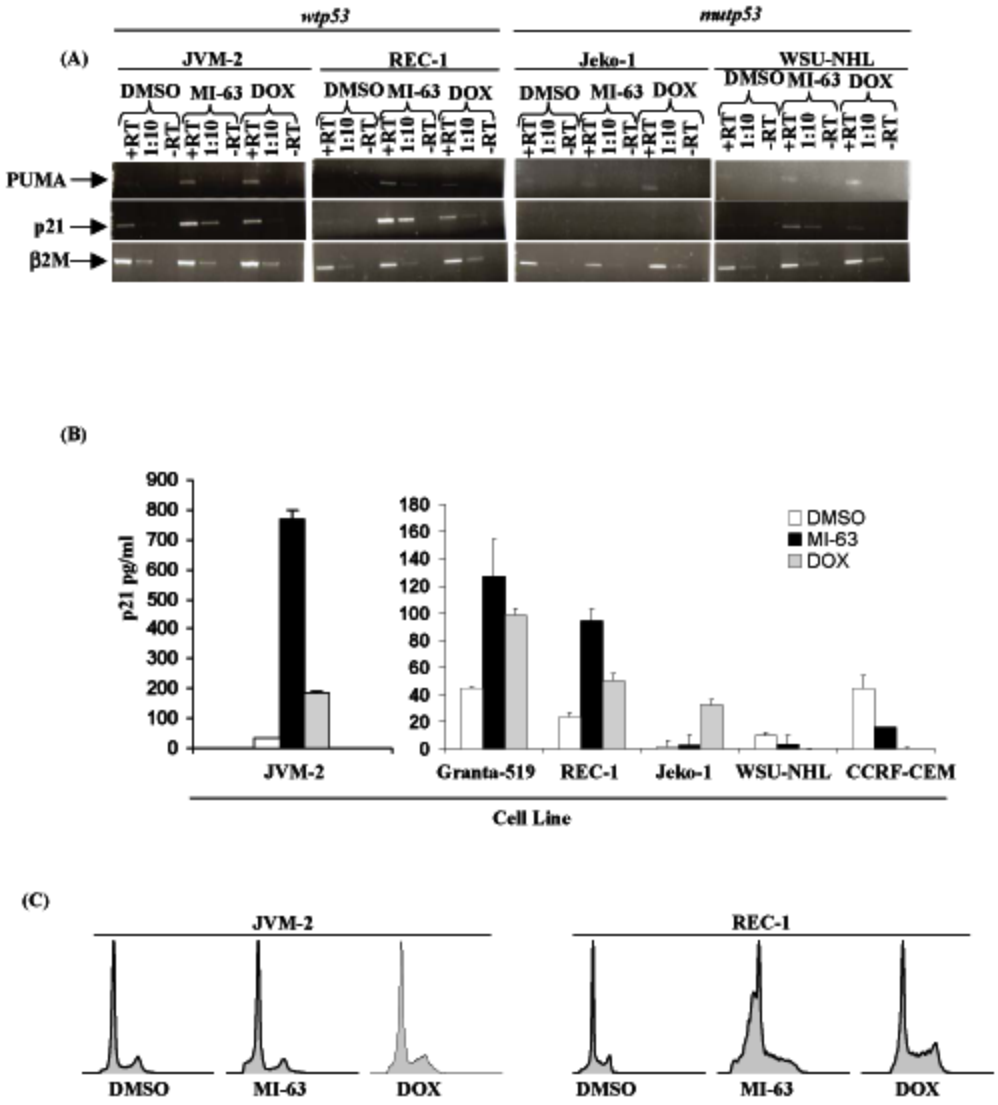

Figure 2. Molecular effects of MI-63 on non-Hodgkin lymphoma cell lines

NHL cell lines were treated with DMSO, 5μM MI-63, or 0.5μM DOX as a positive control for 24 hours. (A) RT-PCR was performed to detect *PUMA* and *p21* mRNA levels, as well as $\beta_2 M$ as a control. Transcripts were visualized by native gel electrophoresis. Lanes marked +RT received 1μl of cDNA stock while those labeled 1:10 received 1μl of a 1:10 dilution of +RT. (B) Cell extracts were probed for their content of p21 using a quantitative ELISA and compared with a standard curve. The levels of p21 are expressed in pg/mL with the mean ± SEM from triplicate experiments. Please note the different scale for JVM-2 cells, which had especially high p21 levels compared with the other cell lines evaluated. (C) Cell cycle analysis was performed of JVM-2, and REC-1, using flow cytometry. Representative profiles of one of the triplicate experiments are shown.

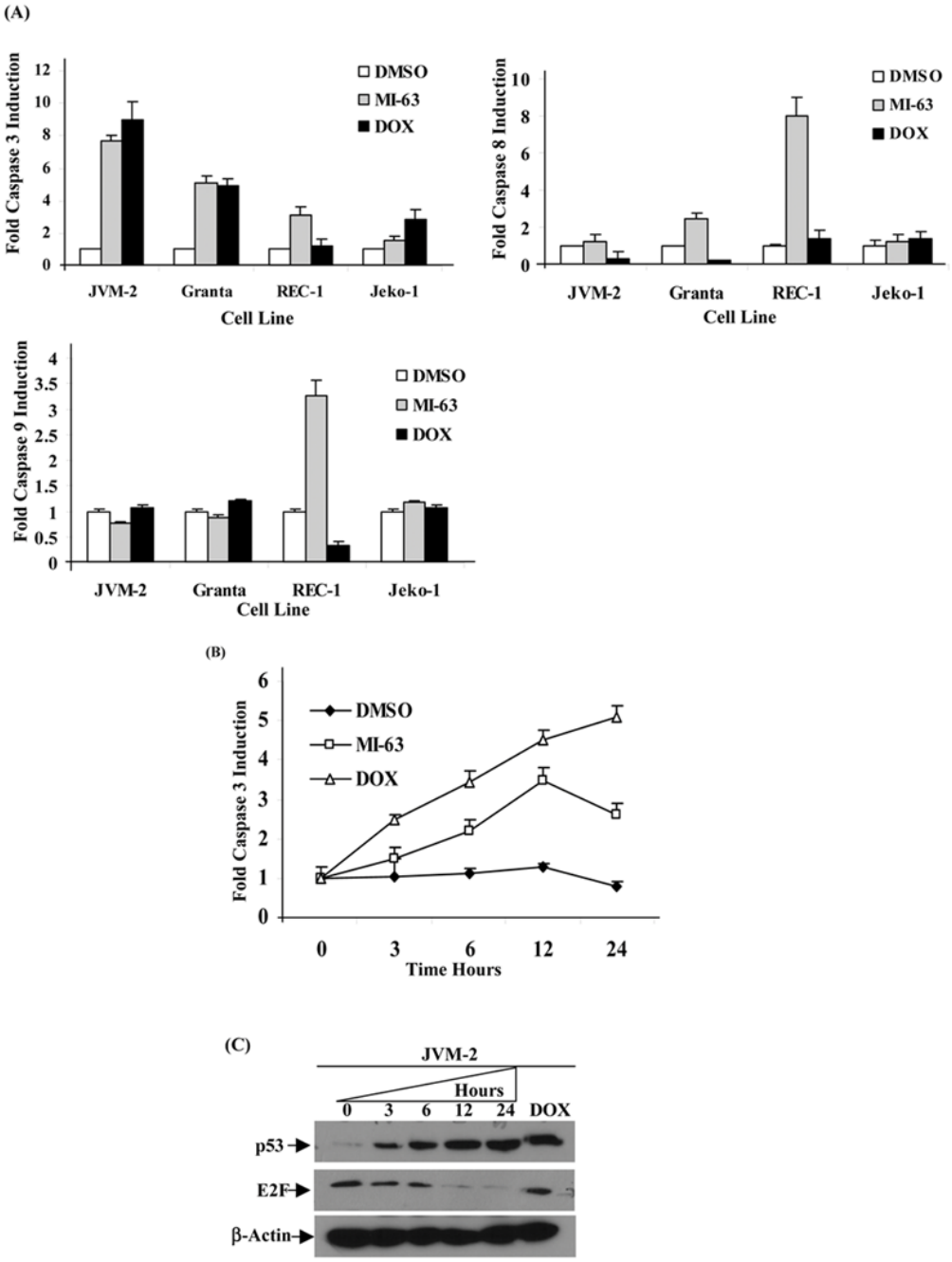

Figure 3. Caspase induction in MCL lines in response to MI-63

(A) MCL cells were treated with DMSO, 5μM MI-63, or 0.5μM DOX for 24 hours. Cellular lysates (50μg/reaction) were then incubated with 40μM fluorogenic substrates specific for caspases-3, 8, and 9. The results are expressed as a fold-caspase activity induction relative to the DMSO control. (B) JVM-2 cells were treated as described above, and lysates prepared at the indicated time points were probed for their caspase-3 activity. (C) JVM-2 cells were treated with MI-63 for the indicated times and then evaluated by Western blotting for their content of p53, E2F1, or β-Actin as a control.

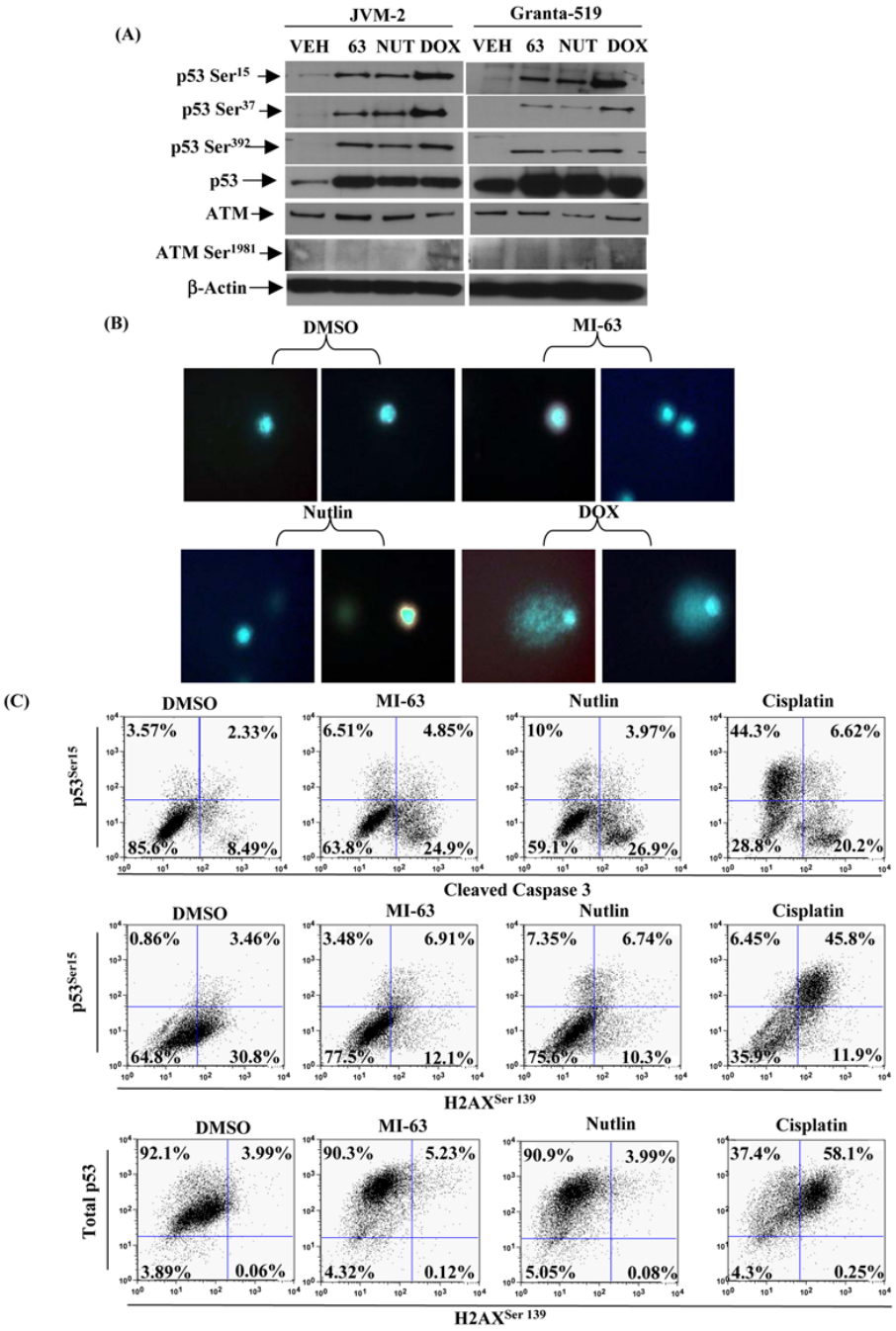

Figure 4. HDM-2 inhibitors induce phosphorylation of p53 and DNA damage

(A) MCL cell lines were treated with DMSO, 5μM MI-63, 5μM nutlin, or 0.5μM doxorubicin for 24 hours, and cellular lysates were probed for their content of p53, as well as several phosphorylated forms of this tumor suppressor, or β-Actin as a control. (B) DNA damage was measured in JVM-2 cells after a 24-hour treatment period with 5μM MI-63, 5μM nutlin, or 0.5μM DOX using the Comet assay, of which two independent panels are shown per drug treatment. (C) JVM-2 cells were treated with DMSO, 5μM MI-63, 5μM nutlin or 5μM cisplatin for 24 hours, and cells were stained for cleaved caspase 3, and phospho-H2AX in combination with either p53-phospho-Ser15 or total p53. Dual color flow cytometry was performed, and

the percentage cells for each quadrant are shown. All experiments shown in this figure were performed in triplicate, and results from a representative experiment are shown.

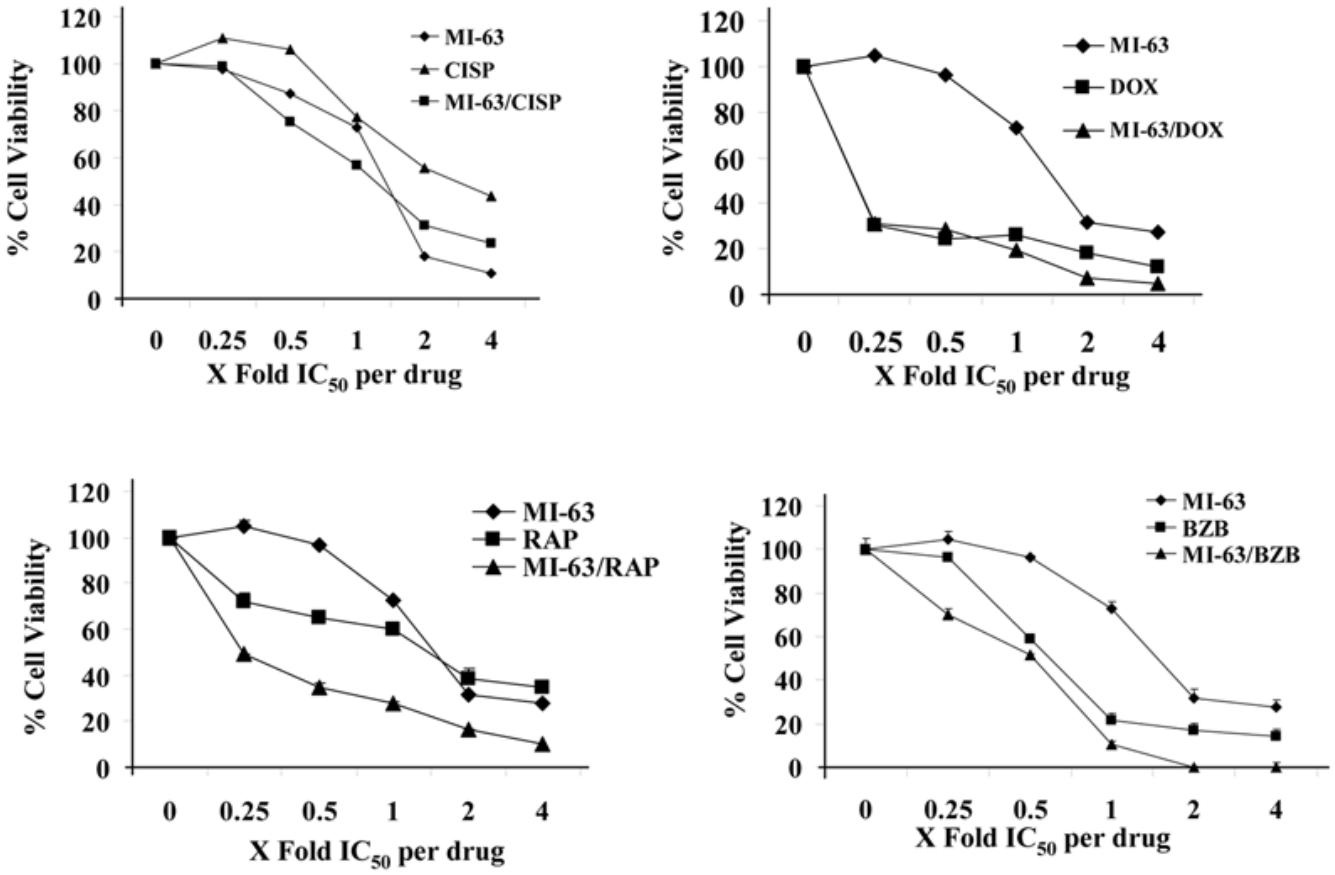

Figure 5. MI-63 synergizes with bortezomib and rapamycin

The IC_{50}′s of cisplatin, doxorubicin, rapamycin, and bortezomib were determined in NHL cell lines, and then matched at a 1:1 ratio with the IC_{50} of MI-63. Cells were treated for 3 days, viability was determined by the WST-1 assay, and results are expressed as the percentage viability in relation to the DMSO control. A viability assay of JVM-2 cells treated with MI-63 alone, or in combination with cisplatin, doxorubicin, rapamycin, or bortezomib is shown. Similar studies were performed with Granta-519, REC-1, WSU-NHL, and CCRF-CEM cells, and used to determine the respective combination indices.

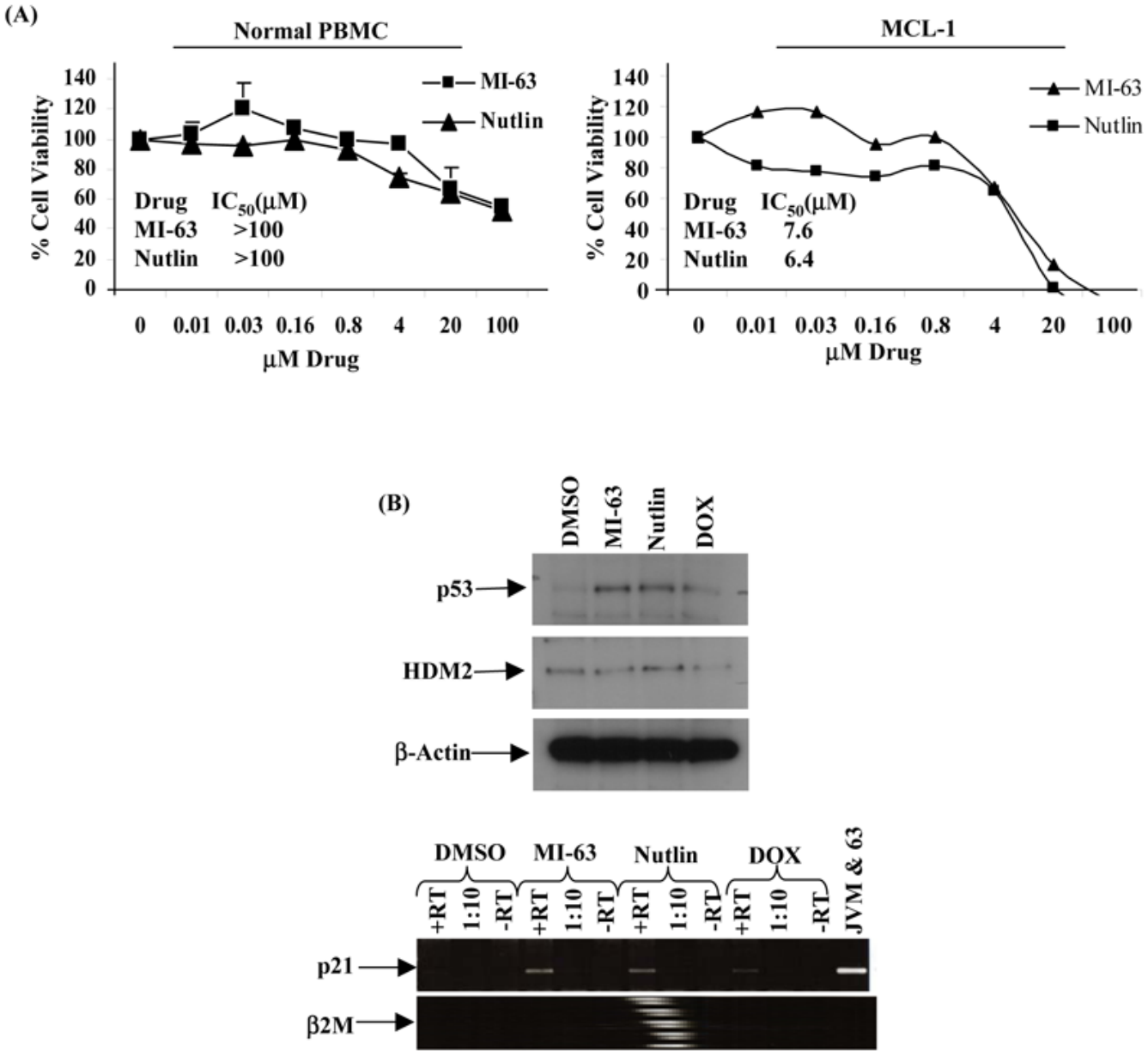

Figure 6. Activity of MI-63 in MCL patient samples

Normal peripheral blood mononuclear cells (PBMC) and peripheral blood from an MCL patient (MCL-1) with blastic phase disease were CD19 column purified to enrich for $CD19^+$ B cells, and then treated with MI-63 or nutlin for 72 hours at the indicated doses. Cell viability was determined using the WST-1 assay. (A) The viability of normal $CD19^+$ B cells from 3 independent patients treated with HDM-2 inhibitors is shown in the left panel. Experiments were performed in triplicate and show SEM. Proliferation of an MCL patient sample is shown on the right. (B) $CD19^+$ B cells from the MCL-1 patient sample were treated with DMSO, 5μM MI-63, or 0.5μM DOX for 24 hours, at which point protein lysates and RNA were collected. Immunoblotting was performed on extracts, which were then probed for their content of p53, HDM-2, and β-Actin. RT-PCR was performed to detect *p21* mRNA levels, and $\beta_2 M$ was used as a control. Transcripts were visualized by native gel electrophoresis. Lanes marked

+RT received 1μl of cDNA stock while those labeled 1:10 received 1μl of a 1:10 dilution of +RT.

Table 1

Combination indices (CI) of NHL cell lines treated with MI-63 and commonly used chemotherapeutic agents

The CI values were calculated after treatments described in Figure 5, and values shown are the mean of triplicate experiments.

Drug (1× IC_{50})	DOX	CISP	BZB	RAP
Cell Line	**CI Values**			
JVM-2	1.0	1.3	0.5	0.4
Granta-519	0.7	0.7	2.1	0.7
REC-1	1.0	0.6	0.6	0.5
WSU-NHL	1.7	0.9	0.3	0.8
CCRF-CEM	0.9	1.0	0.9	0.6